
# Norbornadiene-Quadricyclane Photoswitches with Enhanced Solar Spectrum Match

Chemistry–A European Journal
Research Article
doi.org/10.1002/chem.202401430
Chemistry Europe
European Chemical Societies Publishing
www.chemeurj.org

# Norbornadiene-Quadricyclane Photoswitches with Enhanced Solar Spectrum Match

Adil S. Aslam,[a] Lidiya M. Muhammad,[a] Andreas Erbs Hillers-Bendtsen,[b] Kurt V. Mikkelsen,[b] and Kasper Moth-Poulsen*[a, c, d, e]

*Dedicated to Prof. Dr. Dildar Ahmed on his 64th birthday*

Herein, we report monomeric and dimeric norbornadiene-quadricyclane molecular photoswitch systems intended for molecular solar thermal applications. A series of six new norbornadiene derivatives conjugated with benzothiadiazole as the acceptor unit and dithiafulvene as the donor unit were synthesized and fully characterized. The photoswitches were evaluated by experimentally and theoretically measuring optical absorption profiles and thermal conversion of quadricyclane to norbornadiene. Computational insight by density functional theory calculations at the M06-2X/def2-SVPD level of theory provided geometries, storage energies, UV-vis absorption spectra, and HOMO-LUMO levels that are used to describe the function of the molecular systems. The studied molecules exhibit absorption onset ranging from 416 nm to 595 nm due to a systemic change in their donor-acceptor character. This approach was advantageous due to the introduction of benzothiadiazole and the dimeric nature of molecular structures. The best-performing system has a half-life of 3 days with quantum yields over 50%.

## 1. Introduction

The conversion of solar energy into stored chemical energy is an attractive energy source and has occurred since the beginning of life on our planet. The utilization of stored chemical energy in the form of fossil fuels requires combustion, leading to emissions that are devastating for the environment and global warming. One alternative way to store solar energy in the form of chemical bonds and reversibly release it in a closed cycle is so-called **MO**lecular **S**olar **T**hermal storage systems (MOST).[1] The chemistry of the MOST system is based on (solar) photons that induce photoconversion in a parent photoswitch to a metastable isomer (higher in energy), whereas heat or a catalyst can convert this isomer to the parent photoswitch (low in energy) accompanied by a release of excess energy.

Currently, several molecular systems are being studied for MOST application; examples include stilbene,[2] azobenzenes,[3] Ruthenium fulvalene,[4] Dihydrozoazulenevinylheptafulvene[5] norbornadiene-quadricyclane (NBD/QC) systems,[6] and others.[7] Among these, NBD/QC is receiving attention due to the strained nature of quadricyclane (the metastable isomer possesses a capacity for large energy storage of 96 kJ/mol).[8] They have found applications in device fabrication,[9] adsorption characteristics,[10] ligand chemistry,[11] charge transfer,[12] and battery.[13]

Since unsubstituted NBD only absorbs in the UV region, absorption needs to be red-shifted to furnish a better solar spectrum match, and ideally, the onset of absorption should reach ≈600 nm.[14] There are several examples in the literature on how to move the absorption of NBD into the UV-visible region.[15] Firstly, employing donor/acceptor conjugation on one of the double bonds (Figure 1a),[16] secondly, dimeric NBD systems (Figure 1b),[8,15b,17] and lastly, homoconjugation (through space interaction of donor/acceptor systems, Figure 1c).[18]

Although much work has been carried out with donor/acceptor NBDs, the domain of acceptor/acceptor dimeric NBD systems (Figure 1e) and acceptor/acceptor mono NBD systems (Figure 1f),[17c,19] for application in MOST has not been investigated much. Also, one may speculate if there is a limit to how red-shifted an NBD molecule can be while still fulfilling the requirement of photoswitching. For designing these systems, two factors are at play that should be considered, firstly, the selection of substituents, and secondly, the identification of

[a] A. S. Aslam, L. M. Muhammad, K. Moth-Poulsen
Department of Chemistry and Chemical Engineering, Chalmers University of Technology, SE-41296 Gothenburg, Sweden
[b] A. Erbs Hillers-Bendtsen, K. V. Mikkelsen
Department of Chemistry, University of Copenhagen, Universitetsparken 5, 2100 Copenhagen, Denmark
[c] K. Moth-Poulsen
Department of Chemical Engineering, Universitat Politècnica de Catalunya, Eduard Maristany 10–14, 08019 Barcelona, Spain
E-mail: kasper.moth-poulsen@upc.edu
[d] K. Moth-Poulsen
The Institute of Materials Science of Barcelona, ICMAB-CSIC, Bellaterra, Barcelona 08193, Spain
[e] K. Moth-Poulsen
Catalan Institution for Research & Advanced Studies, ICREA, Pg. Lluís Companys 23, Barcelona, Spain

Supporting information for this article is available on the WWW under https://doi.org/10.1002/chem.202401430

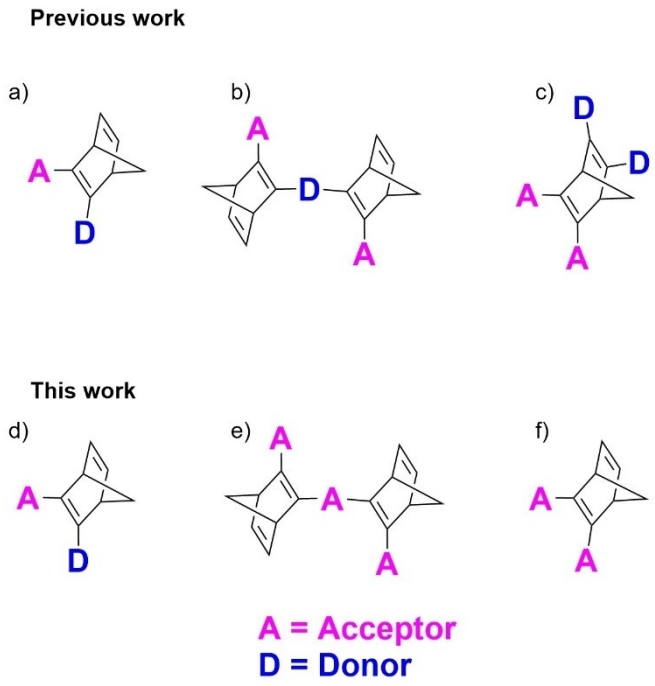


**Figure 1.** Representation of previous work (top) and current work (bottom). (a) donor/acceptor in a double bond pattern, (b) donor/acceptor dimer pattern (NBD/donor/NBD), (c) donor/acceptor through space pattern (Homo-conjugation). (d) donor/acceptor in a double bond pattern (Benzothiadiazole as an acceptor and dithiafulvene as a donor), (e) acceptor/acceptor dimer pattern (NBD/acceptor/NBD), (f) acceptor/acceptor in a double bond pattern.

suitable synthetic routes.[17c,20] As a MOST material, two of the most important factors for efficient solar energy storage are the onset of absorption and the quantum yield, so conjugating with higher molecular weight units can improve solar spectrum match.[17a,21]

For the choice of acceptor unit, we chose benzothiadiazole due to our previous computational study where it was indicated that incorporation of a benzothiadiazole unit as an acceptor would lead to a strong red shift of NBD absorption by shifting the Lowest unoccupied molecular orbital (LUMO) energy.[22] In the study, it was also calculated that the donor group affects the highest occupied molecular orbital (HOMO), so they have a less pronounced effect if compared with acceptor groups, and due to this reason, it is difficult to affect occupied levels as they are coupled to charge density. We note that benzothiadiazole derivatives are widely used in organic solar cells due to their acceptor-type nature and chemical stability.[22b,23]

Typical donor groups used in NBD functionalization have been simple aromatics such as amino or alkoxy-substituted benzenes.[17a,24] Here, we chose Dithiafulvene (DTF), which is a known strong electron donor unit.[25] It has been previously conjugated with Dihydroazulene (DHA) photoswitches through an acetylene spacer.[26] DHA-DTF coupling demonstrated a dominant bathochromic shift in the absorption of both photo-switches. DTF-NBD (direct conjugation) system has not been evaluated so far except with either an acetylenic or phenyl unit.[27]

In summary, we report here the synthesis and characterization of a new series of benzothiadiazole and DTF substituted NBD derivatives with enhanced solar spectrum match profiles leading to insights into NBD/QC functionality and possible limitations (Figure 1d–f).

## 2. Results and Discussion

### 2.1. Synthesis

NBD derivatives have been commonly synthesized using either Diels-Alder or palladium-catalyzed cross-coupling strategies.[15c,17b,24c] We initially set out to synthesize our molecules through the Diels-Alder route (last step) but after failed attempts, we shifted our focus to palladium-catalyzed cross-coupling (Suzuki and Sonogashira coupling or condensation reaction conditions) and with our modified approach we managed to prepare six new **NBDs 1–6** (Schemes 1 and 2).

Firstly, we focused on the synthesis of mono and dimeric/bis NBD systems (see Scheme 1, right). The first crucial intermediate Br-ester NBD was synthesized via a two-step method. The first step was the bromination of ethyl propialate and the second step was a Diels-Alder reaction of Br-ester with freshly cracked cyclopentadiene to give Br-ester NBD using a literature method.[28] Mono-pinacolester benzothiadiazole[29] was coupled to Br-ester NBD via Suzuki coupling to give **NBD 1** in a yield of 32%. Bis-pinacolester benzothiadiazole (prepared using 4,7-Dibromo-2,1,3-benzothiadiazole)[29] was coupled to Br-ester under similar conditions to give **NBD 3** as a dimer (NBD-NBD) in a yield of 24%. Secondly, to explore elongated conjugates another strategy was devised. Mono Br-benzothiadiazole and bis Br-benzothiadiazole were subjected to mono TMS-protected acetylene via Sonogashira coupling to give TMS-protected mono and bis acetylenic benzothiadiazole. It was subjected to a mixture of potassium carbonate in MeOH/THF to remove TMS.[30] Br-ester NBD was coupled with mono and bis acetylenic benzothiadiazole via a Sonogashira coupling to give **NBD 2** in a yield of 33%, and **NBD 4** as a highly conjugated dimer in a yield of 24% (scheme 1, left).

Lastly, the synthetic protocol for the donor/acceptor **NBD 5** and **6** (Figure 1d) system is shown in Scheme 2. Commercially available bromo-benzothiadiazole was coupled with propargyl alcohol using a Sonogashira method to give **7** in a yield of 80%. The primary alcohol was oxidized to aldehyde using $MnO_2$ to give **8** in a yield of 50%. This was subjected to Diels-Alder reaction using freshly cracked cyclopentadiene to give **9** in a yield of 83%. The Diels-Alder adduct was used as a precursor for condensation with two different DTF units in the presence of triethyl phosphite to generate **NBD 5** and **6** in a yield of 25% and 29%, respectively.

### 2.2 Photoconversion

The first and foremost task was to determine the absorption profiles of synthesized NBDs. The UV/Vis absorption profiles of

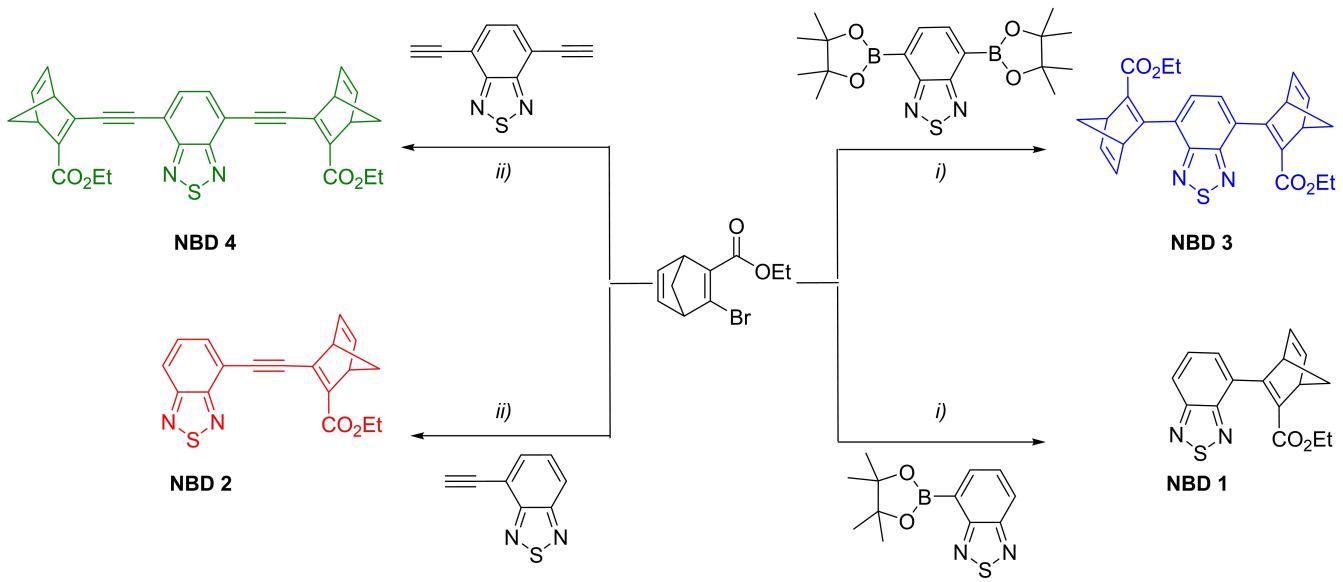


**Scheme 1.** Synthesis of benzothiadiazole functionalized **NBDs 1,2,3** and **4**. Conditions: i) $Pd_2dba_3$,BINAP, *t*-ButONa, SPhos, $K_3PO_4$, Toluene, 100 °C, 20 h; ii) $PdCl_2(PPh_3)_2$, CuI, TEA, THF, rt, 16 h, rt = room temperature.

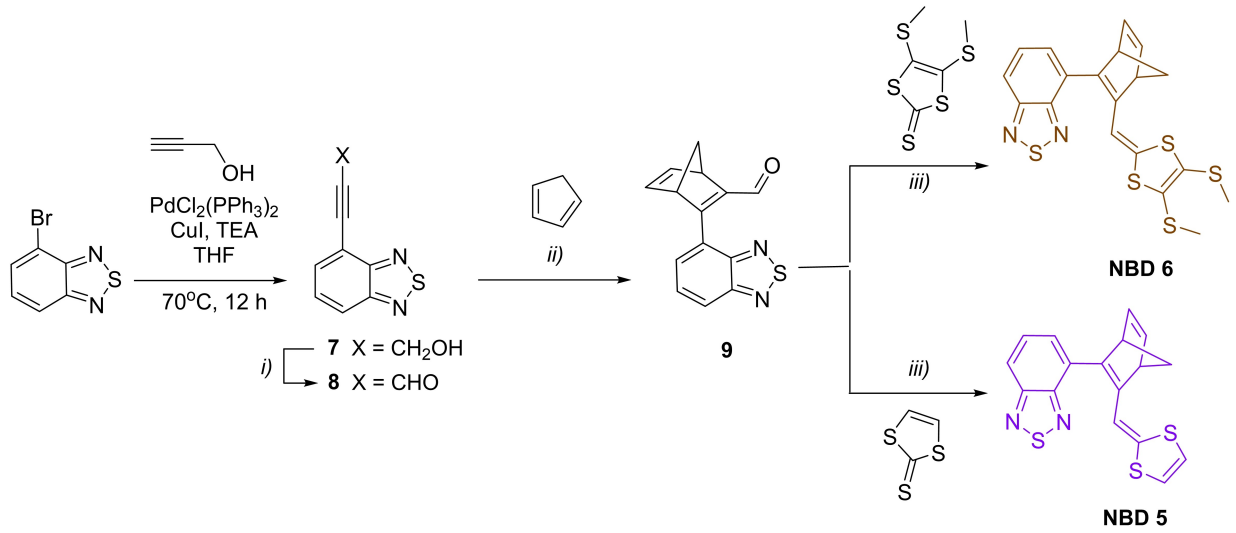


**Scheme 2.** Synthesis of the DTF-benzothiadiazole functionalized **NBD 5** and **6**. Conditions: i) $MnO_2$, DCM, rt, 12 h, ii) Toluene, 110 °C, 16 h, iii) $P(OEt)_3$, 110 °C, 5 h, rt = room temperature.

**NBD 1–6** measured in toluene (Figure 2), absorption onset ($A_{onset}$), maxima, and molar extinction coefficients are summarized in Table 1. The onset absorption for unsubstituted NBD is at 267 nm. The most red-shifted absorption was observed for **NBD 6** with an onset at 595 nm (maxima at 316), whereas the onset for **NBD 1–5** is all found in the range of 416–588 nm. Although **NBD 6** gives a more red-shifted absorption and better solar spectrum match, **NBD 4** has a more distinctive absorption maxima.

The onset for **NBD 1** is at 416 nm (maxima at 315), which is redshifted compared to unsubstituted NBD. When compared with the spectrum of **NBD 2**, which has an onset of 454 nm, it becomes evident that the insertion of an ethynyl unit not only has a significant effect on the absorption but also enhances the

**Table 1.** Absorption onsets, absorption maxima, molar extinction coefficients, and quantum yields of conversion to the corresponding quadricyclanes.

| NBD | $\lambda_{onset}$ [a] (nm) | $\lambda_{max}$ (nm) | $\varepsilon_{max}$ [b] ($M^{-1}cm^{-1}$) | QY% [b] |
|---|---|---|---|---|
| **1** | 416 | 315 | 5470 | 57 |
| **2** | 454 | 320 | 18470 | 15 |
| **3** | 460 | 318 | 7980 | 57 |
| **4** | 510 | 436 | 11840 | – |
| **5** | 588 | 315 | 8690 | – |
| **6** | 595 | 316 | 15330 | 4 |

[a] $A_{onset}$ is defined as log ε = 0.2. [b] measured in toluene.

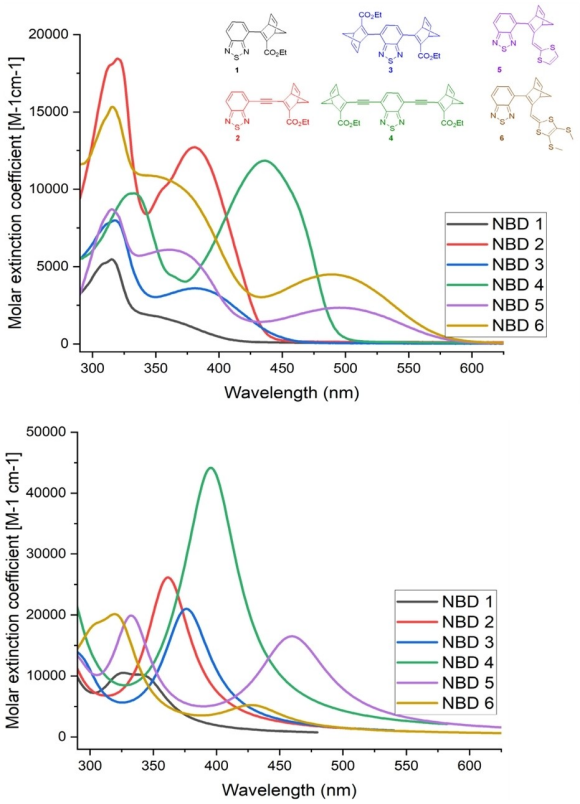


**Figure 2.** Experimental absorption profiles (top): NBD 1 (black line), NBD 2 (red line), NBD 3 (blue line), NBD 4 (green line), NBD 5 (purple line), NBD 6 (brown line). Inset: Molecular structure of synthesized NBDs. Computed absorption profiles (bottom) of NBD 1–6.

extinction coefficient. Moreover, two distinctive maxima were formed. The difference between the absorption onset of **NBD 3** (460 nm) and **NBD 1** (416 nm) was around 45 nm. This could be attributed to the dimeric nature of the compound and a more conjugated system. Upon further investigation of absorption onsets, **NBD 4** gave a more redshifted absorption, with an onset at 510 nm. The introduction of two ethynyl units and enhanced conjugation had a pronounced effect not only on the onset but also on the extinction coefficient (Table 1). After the evaluation of acceptor-acceptor systems, we turned our attention toward the effect of new donor-NBD-acceptor systems. The absorption onset for **NBD 5** (588 nm) and **NBD 6** (595 nm) was the most redshifted. There was a major reduction of the extinction coefficients of **NBD 5** and **NBD 6** as compared to **NBD 2** and **NBD 4**, which had maxima in the visible region. It is to be noted that both **NBD 5** and **NBD 6**, with an absorption close to 600 nm fulfill the optical properties of an" ideal" MOST system.[14]

**NBD 1–6** were exposed to LED light sources (310, 340, 405, 415, and 455 nm) to observe the respective photoproducts **QC 10–15**. The photoisomerization was monitored by UV/Vis spectroscopy. Upon irradiation, spectral overlap (photostationary state) between NBD and QC (Figure S2) was observed for several of the synthesized compounds (Figure 3).[8]

Photoirradiation of **NBD 1** (Figure 3a) at 310 nm led to gradual conversion to the **QC 10**. However, only partial photo-conversion was observed leading to a photostationary state (PSS). NMR spectroscopy confirmed that only 50% conversion could be obtained (see Figure S21). When the NMR sample was heated at 100 °C for 24 h, it converted back to parent NBD, indicating clean back-conversion. **NBD 2** (Figure 3b) was irradiated at 405 nm, and a decrease in absorbance was observed within 10 seconds forming **QC 11**. It reached the PSS within 120 seconds and displayed no further conversion. On the NMR scale, when the sample was irradiated for 2 h at 405 nm, no QC peaks were observed (see Figure S22). Similarly, **NBD 3** (Figure 3c) was subjected to irradiation at 340 nm, leading to a small decrease in absorbance before reaching PSS. Prolonged irradiation did not affect the absorbance. Photoirradiation of the NMR sample resulted in a 15% conversion to **QC 12** (see Figure S23). **NBD 4** (Figure 3d) was irradiated at 405 nm, resulting in a smaller decrease in absorbance, and the sample converted back immediately at room temperature. This was supported by $^{1}$H NMR (see Figure S24), where **QC 13** signals were not observed. Photoirradiation of **NBD 5** (Figure 3e) and **NBD 6** (Figure 3f) at 405 nm gave an isosbestic point at 318 and 319 nm in the UV/Vis, respectively. However, **QC 14** and **15** were not observed.

Photoisomerization quantum yields (QYs) were determined in toluene using potassium ferrioxalate as a chemical actinometer.[31] The experiments were conducted using a 310 nm or 405 nm light-emitting diode. The results, reported in Table 1, are an average of two measurements. The highest quantum yields were observed for **NBD 1** and **NBD 3** at 57%. **NBD 2** had a quantum yield of 15%, while **NBD 6** had the lowest quantum yield of 4% (see Figures S32–35). Unfortunately, the quantum yield for **NBD 4** couldn't be determined due to its quick back conversion.

### 2.3. Back Conversion

Kinetic studies were conducted to determine the thermal stabilities of the QC 10–15 photoisomers and the enthalpies and entropies of activation for the thermally induced back reactions. Rate constants, *k*, at four different temperatures (50 °C, 60 °C, 70 °C, 80 °C) were measured and half-life ($t_{1/2}$) was determined at 25 °C from an Arrhenius analysis revealing both the enthalpy (ΔH) and entropy (ΔS) of the QC to NBD conversion (Table 2).

Photo-irradiated NBDs were heated, and back conversion was measured by studying the increase in absorbance using UV/Vis spectrophotometry (see Figures S29–31). Enthalpies and entropies of activation were estimated using the Eyring equation (Table 2).

From the experiments, it was evident that **QC 10** was very stable, with a half-life of around 35.88 h. Upon introduction of ethynyl bridge, it resulted in **QC 11** where the half-life decreased to 0.8 h. The half-life for **QC 12** was identical to **QC 10** which suggests that only one of the NBDs was photo-converted to QC (NBD-NBD to NBD-QC) rather than conversion of both NBDs to QCs. The half-life for **NBD 4–6** couldn't be determined.

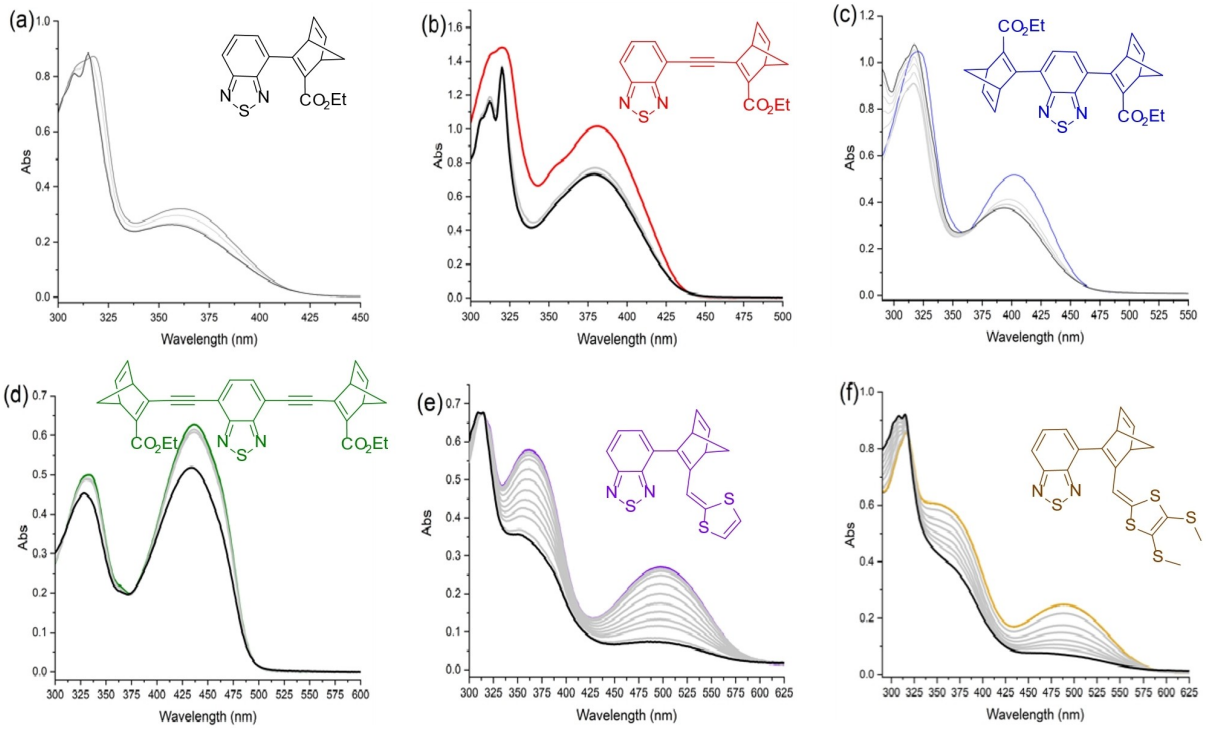


**Figure 3.** UV/Vis absorption spectra of NBDs (1–6) upon photoirradiation recorded in toluene. (a) NBD 1 irradiated at 310 nm, (b) NBD 2 irradiated at 405 nm, (c) NBD 3 irradiated at 340 nm, (d) NBD 4 irradiated at 455 nm, (e) NBD 5 irradiated at 405 nm, (f) NBD 6 irradiated at 405 nm.

**Table 2.** Experimental and computed thermodynamic values of QC to NBD.

| QC to NBD | ΔH (kJ/mol) | ΔS ($JK^{-1}mol^{-1}$) | $t_{1/2}$[a] (h) | First Gibbs free energy (kJ/mol)[b] | First Back reaction barrier (kJ/mol)[b] | Second Gibbs free energy (kJ/mol)[b] | Second Back reaction barrier (kJ/mol)[b] |
|---|---|---|---|---|---|---|---|
| **10** to **1** | 64.104 | −130.7 | 35.88 | 39.76 | 195.98 | – | – |
| **11** to **2** | 53.561 | −134.5 | 0.8 | 51.95 | 196.61 | – | – |
| **12** to **3** | 84.689 | −61.11 | 33.71 | 42.44 | 172.25 | 22.43 | 200.97 |
| **13** to **4** | – | – | – | 38.66 | – | 54.98 | – |
| **14** to **5** | – | – | – | 61.22 | 191.72 | – | – |
| **15** to **6** | – | – | – | 62.21 | 174.70 | – | – |

[a] Half-lives determined from Eyring parameters at 25 °C in toluene. [b] computed values.

The insight into the photophysical properties shed a great amount of light on the advantages of conjugating NBD benzothiadiazole and dithiafulvene in terms of bathochromic shift. The systems suffer from photostationary state and back conversion problems. Insight into energy levels and orbital overlap may help us design better systems using density functional theory (DFT) based modeling.

### 2.4. DFT Studies

For a deeper understanding of **NBD 1–6**, we applied density functional theory at the M06-2X/def2-SVPD level of theory,[32] which has previously been established to give geometries, storage energies, and UV-vis absorption spectra. Initially, we performed geometry optimization of the different isomers (NBD, QC, NBD-NBD, NBD-QC, and QC-QC) of the six compounds as well as the transition states connecting them via thermally activated reactions. Subsequently, we performed frequency calculations on all optimized geometries, and for all minimum energy structures, we determined the 30 lowest vertical excitation energies and associated oscillator strengths, which were converted into UV-vis absorption spectra by convolution using Lorentzian functions with a full-width half maximum of 0.4 eV. All calculations were performed using Orca 5.0[33] program package using the conductor polarizable continuum model[34] for solvation in toluene and the Tamm-Dancoff approximation for the UV-vis calculations. Initially, it is seen that the predicted absorption spectra for the NBD and NBD-NBD forms of the six systems have onset absorption blue-shifted by

20–90 nm (see Figure 2 and Table S1). We note that both the predicted and measured spectra have some similarity in the onset absorption trend (see Table 1 and S1), however, the shapes and absorption maxima differ to some extent which can be seen when comparing the six systems (Figure 2). The calculations further elucidate the spectra of the corresponding **QC10-15** photoproducts (see Figure S36–41). In all cases, switching of the NBD isomer leads to a blueshift and decrease in absorption. However, it is only for **NBD 5** (Figure 4a) that the first absorption band is predicted to diminish entirely upon photoswitching, while the five other systems have a significant overlap between NBD and QC absorption. This observation indicates that only **NBD 5** has the NBD core fully involved in the excitation underlying the first absorption band (see Figure S40) and this explains why the spectral changes observed for systems **NBD 1–4** and **6** after photoswitching appear insignificant. This provides a possible explanation for the partial conversion of systems **NBD 1–4** given that reverse photoswitching of the QC isomer can happen due to competing absorption from both NBD and QC species leading to photostationary states.

To further analyze the inability of full photoconversion, we calculated HOMO-LUMO levels. The lowest transition orbitals in each of the orbitals for NBDs (see Table SI 3) display a very delocalized LUMO, which could be an indication that the systems have their lowest absorption being a Rydberg transition. This could be a plausible explanation for the lack of photoswitching in systems **NBD 5** and **6** (Figure 4).

Most crucially, the calculations correctly capture all the trends, namely the increasing redshift from **NBD 1** to **6**. Computational spectra clearly highlight stepwise blue shift for dimers (**NBD 3** and **NBD 4**) due to stepwise conversion of both NBDs. Although, experimentally we have observed conversion of only one NBD to QC in dimers, whereas stepwise conversion in dimers has been demonstrated previously.[17b] Another similarity between the experimental and computed values is the large difference in the magnitude of the extinction coefficient between equivalent compounds with an ethynyl bridge (**NBD 2** and **NBD 4**) and dimers (**NBD 1** and **NBD 3**). We predicted thermochemical properties using the obtained data. We determined the theoretical upper limit of solar conversion efficiency of each compound using the storage energies, thermal back reaction barriers, and UV-vis data obtained from DFT (see SI Table 2). **NBD 5** and **6** gave a value of 1.15 and 0.72%, respectively. This was due to the excellent solar spectrum match of **NBD 5** and **6**. The values for **NBD 1–4** were in a range from 0.16% to 0.5%. Low predicted solar conversion efficiencies are likely correlated to the expectation that the back reaction barriers are overestimated due to our choice of DFT methodology.

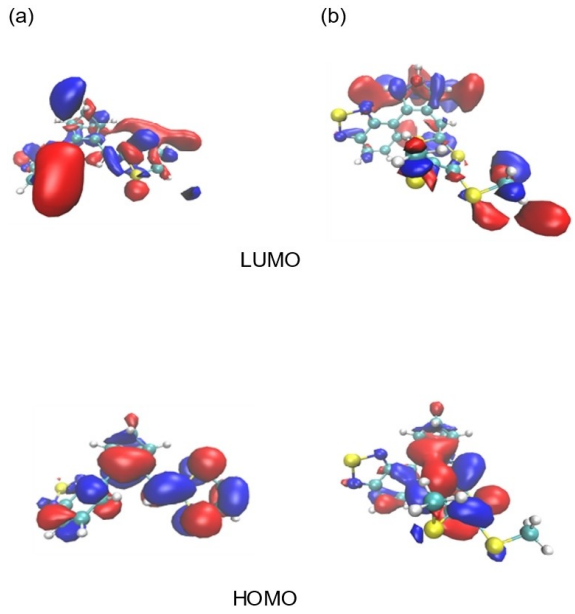


**Figure 4.** Transition orbitals of (a) NBD 5 and (b) NBD 6.

## 3. Conclusions

A series of NBDs conjugated with benzothiadiazole as acceptor and dithiafulvene as donor units have been synthesized and evaluated in the context of better solar spectrum match. It includes mono and bis NBDs. Suzuki and Sonogashira couplings have been utilized to synthesize the desired compounds.

We observed half-lives (0.8 h to 35.8 h) and quantum yields (4% to 57%), respectively. The strategy of mono and bis NBDs has displayed not only the advantage of increasing wavelength (absorbance onset 416–595 nm) but also higher molar extinction coefficients. Overall, a redshift of more than 330 nm compared to unsubstituted NBD (267 nm) was achieved in **NBD 6**. The acceptor/acceptor dimeric NBD (NBD-NBD) displayed absorbance onset at 510 nm, whereas the introduction of dithiafulvene pushed the onset to 595 nm, which is within the target of 590–650 nm put forward in previous works,[14] indicating the pronounced effect of the synthetic strategy.

The synthesized systems shine a light on the challenges of competing/overlapping absorption for the QCs, which result in partial photoisomerization of the NBD system. Due to these factors, the full potential of these NBDs couldn't be explored. Hence, more effort towards molecular engineering and design is needed to enhance the efficiency of MOST systems in the future.

## Experimental Section

### Methods

All commercial chemicals were used as received. Toluene was dried on an MBraun MB SPS-800 solvent purification system. Column chromatography was performed on a Biotage Isolera One instrument using pre-packed silica columns (10 g, 25 g, or 50 g Biotage® SNAP Cartridge). Cyclopentadiene was distilled by cracking dicyclopentadiene over iron filings and stored at −-80 °C. Thin layer chromatography (TLC) was carried out using aluminum sheets precoated with silica gel. $^{1}$H NMR (400 MHz) and $^{13}$C NMR (101 MHz) spectra were recorded on a Varian 400 MHz instrument, or $^{1}$H NMR (600 MHz) and $^{13}$C NMR (151 MHz) spectra were recorded on a Bruker 600 MHz instrument, using the residual solvent as the

internal standard ($CDCl_3$, $^1H = 7.26$ ppm and $^{13}C = 77.16$ ppm, or $CD_3CN$, $^1H = 1.94$ ppm). All NMR experiments were acquired at 298 K unless specified. All chemical shifts are quoted on the δ scale (ppm), and all coupling constants (J) are expressed in Hz. All solution-based spectroscopic measurements were performed in a 1 cm path length cuvette on either a Cary 60 Bio or a Cary 100 UV–vis spectrophotometer, scanning the wavelength from 700 to 300 nm coupled with Peltier temperature control.

### *NBD 1*

4-(4,4,5,5-tetramethyl-1,3,2-dioxaborolan-2-yl) benzo [c] [1,2,5] thiadiazole (100 mg, 0.38 mmol, 1 eq.), ethyl 3-bromobicyclo[2.2.1] hepta-2,5-diene-2-carboxylate (185.49 mg, 0.76 mmol, 2 eq.), anhydrous $K_3PO_4$ (648.1 mg, 3.05 mmol, 8 eq.), Sphos (6.26 mg, 0.015 mmol, 0.04 eq.) and toluene (4 mL) were added to a round bottom flask. The mixture was purged with $N_2$, followed by the addition of a mixture of catalysts ($Pd_2dba_3$/ BINAP/ *t*-ButONa, 27.96 mg, 0.030 mmol, 0.08 eq.). The reaction mixture was heated at 100 °C for 20 h, and the progress was monitored by TLC. The reaction mixture was cooled to rt, and the solvent was evaporated. The crude product was purified over automated flash chromatography by gradient elution to obtain **NBD 1** (37 mg, 32%). $R_f = 0.2$ (EtOAc/Hexane 0–10%); $^1H$ NMR (400 MHz, $CDCl_3$): δ = 7.94 (dd, *J* = 8.7, 1.2 Hz, 1H), 7.64 (dd, *J* = 7.0, 1.2 Hz, 1H), 7.57 (dd, *J* = 8.7, 7.0 Hz, 1H), 7.11–7.02 (m, 2H), 4.17–4.08 (m, 2H), 4.03 (qd, *J* = 7.1, 0.8 Hz, 2H), 2.44 (dt, *J* = 6.6, 1.7 Hz, 1H), 2.17 (dt, *J* = 6.7, 1.6 Hz, 1H), 1.03 (t, *J* = 7.1 Hz, 3H); $^{13}C$ NMR (101 MHz, $CDCl_3$): δ = 165.29, 163.16, 154.96, 153.02, 143.74, 143.22, 142.36, 129.60, 128.97, 128.56, 121.23, 71.54, 60.12, 58.46, 52.50, 13.94; HRMS (ESI+) m/z: $[M+H]^+$ calcd. for $C_{16}H_{14}N_2O_2S$: 299.0854; found: 299.0851.

### *NBD 2*

To a round bottom flask ethyl 3-bromobicyclo[2.2.1]hepta-2,5-diene-2-carboxylate (170 mg, 0.69 mmol, 1 eq.), $Pd(PPh_3)_2Cl_2$ (24.5 mg, 0.03 mmol, 0.05 eq.) and CuI (6.65 mg, 0.03 mmol, 0.05 eq.) were added followed by addition of anhydrous THF (8 mL). Purged with $N_2$ for 10 mins followed by $Et_3N$ (1.5 mL) and 4-ethynylbenzo[c][1,2,5]thiadiazole (111.8 mg, 0.69 mmol, 1 eq.) addition. The reaction mixture was heated at 70 °C for 16 h, and reaction progress was monitored by TLC. The mixture was cooled to rt, poured into $H_2O$ (100 mL), and extracted with EtOAc (3×25 mL). The crude product was purified over automated flash chromatography by gradient elution to obtain **NBD 2** (75 mg, 33.3%) as a yellow solid. $R_f = 0.3$ (EtOAc/Hexane 0–10%); m.p. 63 °C; $^1H$ NMR (600 MHz, $CDCl_3$): δ = 7.94 (dd, *J* = 8.8, 1.0 Hz, 1H), 7.72 (dd, *J* = 7.0, 1.0 Hz, 1H), 7.52 (dd, *J* = 8.8, 7.0 Hz, 1H), 6.91–6.76 (m, 2H), 4.29–4.13 (m, 2H), 4.01 (dh, *J* = 2.5, 1.3 Hz, 1H), 3.87 (tq, *J* = 2.5, 1.3 Hz, 1H), 2.26 (dt, *J* = 6.8, 1.7 Hz, 1H), 2.11 (dt, *J* = 6.8, 1.6 Hz, 1H), 1.28 (t, *J* = 7.1 Hz, 3H); $^{13}C$ NMR (151 MHz, $CDCl_3$): δ = 164.11, 154.62, 154.20, 151.17, 146.86, 142.73, 141.46, 133.07, 129.21, 122.41, 117.03, 101.22, 91.49, 72.14, 60.66, 58.38, 51.53, 14.42; HRMS (ESI+) m/z: $[M+H]^+$ calcd. for $C_{18}H_{14}N_2O_2S$: 323.0854; found: 323.0863.

### *NBD 3*

4,7-bis(4,4,5,5-tetramethyl-1,3,2-dioxaborolan-2-yl) benzo [c] [1,2,5] thiadiazole (100 mg, 0.25 mmol, 1 eq.), ethyl 3-bromobicyclo [2.2.1] hepta-2,5-diene-2-carboxylate (250 mg, 1.03 mmol, 4 eq.), anhydrous $K_3PO_4$ (437.6 mg, 2.06 mmol, 8 eq.), Sphos (4.23 mg, 0.01 mmol, 0.04 eq.) and toluene (4 mL) were added to a round bottom flask. The mixture was purged with $N_2$, followed by the addition of a mixture of catalysts ($Pd_2dba_3$/BINAP/*t*-ButONa, 21.24 mg, 0.02 mmol, 0.09 eq.). The reaction mixture was heated at 100 °C for 20 h and the progress was monitored by TLC. The mixture was cooled to rt and the solvent was evaporated. The crude product was purified over automated flash chromatography by gradient elution to obtain **NBD 3** (30 mg, 24%). $R_f = 0.3$ (EtOAc/Hexane 0–10); $^1H$ NMR (400 MHz, $CDCl_3$): δ = 7.68 (s, 1H), 7.64 (s, 1H), 7.09–7.02 (m, 4H), 4.12 (dqq, *J* = 5.4, 2.6, 1.2 Hz, 5H), 4.09–4.02 (m, 4H), 2.42 (ddt, *J* = 8.3, 6.6, 1.7 Hz, 2H), 2.18–2.14 (m, 2H), 1.09 (td, *J* = 7.1, 3.7 Hz, 7H); $^{13}C$ NMR (101 MHz, $CDCl_3$): δ = 165.30, 163.21, 163.10, 153.13, 143.80, 143.77, 143.19, 143.06, 142.45, 142.36, 129.22, 129.15, 128.52, 128.32, 71.47, 71.32, 60.14, 58.41, 52.58, 52.54, 14.06, 14.04; HRMS: (ESI+) m/z: $[M+H]^+$ calcd. for $C_{26}H_{24}N_2O_4S$: 461.1535; found: 461.1523.

### *NBD 4*

To a round bottom flask ethyl 3-bromobicyclo[2.2.1]hepta-2,5-diene-2-carboxylate (792.3 mg, 3.26 mmol, 4 eq.), $Pd(PPh_3)_2Cl_2$ (22.8 mg, 0.03 mmol, 0.04 eq.) and CuI (10.86 mg, 0.05 mmol, 0.07 eq.) were added followed by anhydrous THF (8 mL). $Et_3N$ (10 mL) was added. The reaction mixture was purged with $N_2$ for 10 mins followed by the addition of 4,7-diethynylbenzo[c][1,2,5]thiadiazole (150 mg, 0.81 mmol, 1 eq.). Then it was heated at 70 °C for 16 h and the progress was monitored by TLC. The mixture was cooled to rt then poured into $H_2O$ (100 mL) and extracted with EtOAc (3×25 mL). The crude product was purified over automated column chromatography to obtain **NBD 4** (100 mg, 24.1%) as a bright yellow thick oil. $R_f = 0.35$ (EtOAc/Hexane 30%); $^1H$ NMR (600 MHz, $CDCl_3$): δ = 7.76 (s, 2H), 6.91 (tdd, *J* = 5.1, 4.2, 2.6 Hz, 4H), 4.32–4.28 (m, 3H), 4.08 (td, *J* = 2.8, 1.2 Hz, 2H), 3.94 (dd, *J* = 2.8, 1.5 Hz, 2H), 2.33 (dt, *J* = 6.9, 1.7 Hz, 2H), 2.19 (dt, *J* = 6.9, 1.6 Hz, 2H), 1.35 (t, *J* = 7.1 Hz, 6H); $^{13}C$ NMR (151 MHz, $CDCl_3$): δ = 164.01, 154.01, 151.78, 146.65, 142.72, 141.47, 132.79, 117.53, 101.33, 93.58, 72.19, 60.71, 58.33, 51.60, 14.42; HRMS (ESI+) m/z: $[M+H]^+$ calcd. for $C_{30}H_{24}N_2O_4S$: 509.1535; found: 509.1556.

### *NBD 5*

To a round bottom flask, compound **9** (100 mg, 0.37 mmol, 1 eq.), 1,3-dithiole-2-thione (75 mg, 0.56 mmol, 1.5 eq.), and $P(OEt)_3$ (3 mL) were added. The mixture was heated at 110 °C under an Ar atmosphere for 5 h. $P(OEt)_3$ was evaporated, and the crude product was purified over column chromatography to obtain **NBD 5** (37 mg, 29%) as a dark red solid. $R_f = 0.4$ (EtOAc/Hexane 15%); $^1H$ NMR (400 MHz, $CDCl_3$) δ = 7.81 (dd, *J* = 8.8, 1.0 Hz, 1H), 7.54 (dd, *J* = 8.8, 7.0 Hz, 1H), 7.28 (dd, *J* = 7.0, 1.0 Hz, 1H), 7.12 (dt, *J* = 5.0, 1.8 Hz, 1H), 6.86 (ddd, *J* = 5.3, 2.9, 0.8 Hz, 1H), 6.50 (t, *J* = 0.9 Hz, 1H), 6.22 (dd, *J* = 2.6, 1.0 Hz, 1H), 4.42 (t, *J* = 2.3 Hz, 1H), 4.20 (dh, *J* = 3.7, 1.1 Hz, 1H), 2.30 (dt, *J* = 6.5, 1.7 Hz, 1H), 2.17 (dt, *J* = 6.4, 1.7 Hz, 1H); $^{13}C$ NMR (101 MHz, $CDCl_3$) δ = 155.72, 153.65, 150.19, 144.66, 143.98, 142.26, 136.97, 131.46, 129.69, 126.79, 119.10, 118.43, 117.80, 108.87, 69.50, 55.35, 51.78; HRMS (ESI+) m/z: $[M+H]^+$ calcd. for $C_{17}H_{12}N_2S_3$: 340.021; found: 340.023.

### *NBD 6*

To a round bottom flask, compound **9** (158 mg, 0.62 mmol, 1 eq.), 4,5-bis(methylthio)-1,3-dithiole-2-thione (281.6 mg, 1.24 mmol, 2 eq.) and $P(OEt)_3$ (3 mL) were added. The mixture was heated at 110 °C under an Ar atmosphere for 5 h. $P(OEt)_3$ was evaporated, and the crude product was purified over column chromatography to obtain **NBD 6** (67.5 mg, 25%) as a dark red solid. $R_f = 0.4$ (EtOAc/Hexane 5%); $^1H$ NMR (400 MHz, $CDCl_3$) δ = 7.82 (dd, *J* = 8.6, 1.0 Hz, 1H), 7.57–7.42 (m, 1H), 7.29–7.23 (m, 1H), 7.10 (dd, *J* = 5.1, 3.0 Hz, 1H), 6.86 (dd, *J* = 5.1, 3.1 Hz, 1H), 6.40 (s, 1H), 4.33 (t, *J* = 2.4 Hz, 1H),

4.19 (t, $J=2.4$ Hz, 1H), 2.42–2.35 (m, 6H), 2.29 (dt, $J=6.6$, 1.6 Hz, 1H), 2.17 (dt, $J=6.6$, 1.7 Hz, 1H); $^{13}C$ NMR (101 MHz, $CDCl_3$) $\delta=$ 155.68, 153.55, 149.56, 146.18, 143.86, 142.20, 132.16, 131.23, 129.59, 127.59, 126.88, 125.21, 119.39, 110.78, 69.63, 55.38, 51.94, 19.15, 18.94; HRMS (ESI+) m/z: $[M+H]^+$ calcd. for $C_{19}H_{16}N_2S_5$: 432.9995; found: 432.9995.

**(1R,4S)-3-(benzo[c][1,2,5]thiadiazol-4-yl)bicyclo[2.2.1]hepta-2,5-diene-2-carbaldehyde 9**

To a microwave vial compound **8** (150 mg, 0.79 eq.), freshly cracked cyclopentadiene (210.6 mg, 3.19 mmol, 4 eq.), and toluene (2 mL) were added. It was sealed and heated at 110 °C for 12 h. The mixture was cooled to room temperature and concentrated. The crude product was loaded onto silica gel and purified using automated column chromatography to obtain **9** (170 mg, 83 %) as a light-yellow solid. $R_f=0.4$ (EtOAc/Hexane 15 %); m.p. 85 °C; $^1H$ NMR (400 MHz, $CDCl_3$): $\delta=9.84$ (s, 1H), 8.03 (dd, $J=8.8$, 1.1 Hz, 1H), 7.62 (dd, $J=8.8$, 6.9 Hz, 1H), 7.51 (dd, $J=6.9$, 1.1 Hz, 1H), 7.13–6.91 (m, 2H), 4.35–4.12 (m, 2H), 2.31 (ddt, $J=51.5$, 6.9, 1.6 Hz, 2H); $^{13}C$ NMR (101 MHz, $CDCl_3$): $\delta=186.94$, 171.27, 155.18, 152.91, 152.51, 143.33, 142.25, 129.05, 128.85, 128.14, 122.53, 70.89, 57.82, 48.45. HRMS (ESI+) m/z: $[M+H]^+$ calcd. for $C_{14}H_{10}N_2OS$: 255.055; found: 255.059.

## Supporting Information Summary

The authors have cited additional references within the Supporting Information.[22b,35] Characterization data, theoretical calculations, and $^1H$ and $^{13}C$ NMR spectra for all new compounds are available in the supporting information.

## *Acknowledgements*

This work was supported by the Swedish Energy Agency, the Göran Gustafsson Foundation, the Swedish Research Council, Swedish Research Council Formas, the European Research Council (ERC) under grant agreement CoG, PHOTHERM-101002131, the Catalan Institute of Advanced Studies (ICREA), and the European Union's Horizon 2020 Framework Programme under grant agreement no. 951801 MOST, European Commission (Grant No.765739), the Danish Council for Independent Research, DFF-0136-00081B.

## *Conflict of Interests*

The authors declare no conflict of interest.

## *Data Availability Statement*

The data that support the findings of this study are available in the supplementary material of this article.

**Keywords:** Benzothiadiazole · Dithiafulvene · Norbornadiene · Photoswitches · Redshift

[1] R. J. Salthouse, K. Moth-Poulsen, *J. Mater. Chem. A* **2024**, *12*, 3180–3208.
[2] D. H. Waldeck, *Chem. Rev.* **1991**, *91*, 415–436.
[3] M. Le, G. G. D. Han, *Acc. Mater. Res.* **2022**, *3*, 634–643.
[4] K. Börjesson, A. Lennartson, K. Moth-Poulsen, *J. Fluor. Chem.* **2014**, *161*, 24–28.
[5] E. M. Arpa, B. Durbeej, *Chem. Methods* **2023**, *3*, e202200060.
[6] a) Z. Wang, P. Erhart, T. Li, Z.-Y. Zhang, D. Sampedro, Z. Hu, H. A. Wegner, O. Brummel, J. Libuda, M. B. Nielsen, K. Moth-Poulsen, *Joule* **2021**, *5*, 3116–3136; b) P. Lorenz, A. Hirsch, *Chem. Eur. J.* **2020**, *26*, 5220–5230.
[7] K. Edel, X. Yang, J. S. A. Ishibashi, A. N. Lamm, C. Maichle-Mössmer, Z. X. Giustra, S.-Y. Liu, H. F. Bettinger, *Angew. Chem. Int. Ed.* **2018**, *57*, 5296–5300.
[8] M. Mansø, A. U. Petersen, Z. Wang, P. Erhart, M. B. Nielsen, K. Moth-Poulsen, *Nat. Commun.* **2018**, *9*, 1945.
[9] a) A. Lennartson, A. Roffey, K. Moth-Poulsen, *Tetrahedron Lett.* **2015**, *56*, 1457–1465; b) G. F. Martins, B. D. P. Cardoso, N. Galamba, B. J. C. Cabral, *Energy Fuels* **2023**, *37*, 1731–1756.
[10] F. Hemauer, U. Bauer, L. Fromm, C. Weiß, A. Leng, P. Bachmann, F. Düll, J. Steinhauer, V. Schwaab, R. Grzonka, A. Hirsch, A. Görling, H.-P. Steinrück, C. Papp, *ChemPhysChem* **2022**, *23*, e202200199.
[11] Q. Liu, H. Duan, X. Luo, Y. Tang, G. Li, R. Huang, A. Lei, *Adv. Synth. Catal.* **2008**, *350*, 1349–1354.
[12] a) W. Zika, A. Leng, R. Weiß, S. Pintér, C. M. Schüßlbauer, T. Clark, A. Hirsch, D. M. Guldi, *Chem. Sci.* **2023**, *14*, 11096–11104; b) W. Alex, P. Lorenz, C. Henkel, T. Clark, A. Hirsch, D. M. Guldi, *J. Am. Chem. Soc.* **2022**, *144*, 153–162.
[13] P. Lorenz, T. Luchs, A. Hirsch, *Chem. Eur. J.* **2021**, *27*, 4993–5002.
[14] K. Börjesson, A. Lennartson, K. Moth-Poulsen, *ACS Sustain. Chem. Eng.* **2013**, *1*, 585–590.
[15] a) V. A. Bren, V. I. Minkin, A. D. Dubonosov, V. A. Chernoivanov, V. P. Rybalkm, G. S. Borodkin, *Mol. Cryst. Liq. Cryst. Sci. Technol. Sect. A. Mol. Cryst. Liq. Cryst.* **1997**, *297*, 247–253; b) R. Schulte, S. Afflerbach, T. Paululat, H. Ihmels, *Angew. Chem. Int. Ed.* **2023**, *62*, e202309544; c) J. Orrego-Hernández, A. Dreos, K. Moth-Poulsen, *Acc. Chem. Res.* **2020**, *53*, 1478–1487.
[16] M. Quant, A. Lennartson, A. Dreos, M. Kuisma, P. Erhart, K. Börjesson, K. Moth-Poulsen, *Chem. Eur. J.* **2016**, *22*, 13265–13274.
[17] a) M. Mansø, B. E. Tebikachew, K. Moth-Poulsen, M. B. Nielsen, *Org. Biomol. Chem.* **2018**, *16*, 5585–5590; b) A. U. Petersen, A. I. Hofmann, M. Fillols, M. Mansø, M. Jevric, Z. Wang, C. J. Sumby, C. Müller, K. Moth-Poulsen, *Adv. Sci.* **2019**, *6*, 1900367; c) Y. Harel, A. W. Adamson, C. Kutal, P. A. Grutsch, K. Yasufuku, *J. Phys. Chem.* **1987**, *91*, 901–904; d) R. R. Weber, C. N. Stindt, A.-L. M. J. van der Harten, B. L. Feringa, *Chem. Eur. J.* **2024**, *n/a*, e202400482.
[18] M. Sadao, A. Yoshinobu, Y. Zen-ichi, *Chem. Lett.* **1987**, *16*, 195–198.
[19] R. D. Chambers, A. J. Roche, M. H. Rock, *J. Chem. Soc. Perkin Trans. 1* **1996**, 1095–1100.
[20] a) E. Dalkılıç, A. Daştan, *Tetrahedron* **2015**, *71*, 1966–1970; b) D. Hallooman, L. Rhyman, E. Dalkılıç, A. Daştan, M. I. Elzagheid, L. R. Domingo, P. Ramasami, *ChemistrySelect* **2021**, *6*, 9806–9813.
[21] Z. Wang, H. Hölzel, K. Moth-Poulsen, *Chem. Soc. Rev.* **2022**, *51*, 7313–7326.
[22] a) J. D. Yuen, J. Fan, J. Seifter, B. Lim, R. Hufschmid, A. J. Heeger, F. Wudl, *J. Am. Chem. Soc.* **2011**, *133*, 20799–20807; b) M. Kuisma, A. Lundin, K. Moth-Poulsen, P. Hyldgaard, P. Erhart, *ChemSusChem* **2016**, *9*, 1786–1794.
[23] J. Chen, Y. Cao, *Acc. Chem. Res.* **2009**, *42*, 1709–1718.
[24] a) M. Jevric, A. U. Petersen, M. Mansø, S. Kumar Singh, Z. Wang, A. Dreos, C. Sumby, M. B. Nielsen, K. Börjesson, P. Erhart, K. Moth-Poulsen, *Chem. Eur. J.* **2018**, *24*, 12767–12772; b) M. Jevric, Z. Wang, A. U. Petersen, M. Mansø, C. J. Sumby, M. B. Nielsen, K. Moth-Poulsen, *Eur. J. Org. Chem.* **2019**, *2019*, 2354–2361; c) J. Orrego-Hernández, H. Hölzel, M. Quant, Z. Wang, K. Moth-Poulsen, *Eur. J. Org. Chem.* **2021**, *2021*, 5337–5342.
[25] M. R. Bryce, *Adv. Mater.* **1999**, *11*, 11–23.
[26] M. Åxman Petersen, L. Zhu, S. H. Jensen, A. S. Andersson, A. Kadziola, K. Kilså, M. Brøndsted Nielsen, *Adv. Funct. Mater.* **2007**, *17*, 797–804.
[27] M. Mansø, M. D. Kilde, S. K. Singh, P. Erhart, K. Moth-Poulsen, M. B. Nielsen, *Phys. Chem. Chem. Phys.* **2019**, *21*, 3092–3097.
[28] J. D. Rainier, Q. Xu, *Org. Lett.* **1999**, *1*, 27–30.
[29] S. Liu, H. Zhang, Y. Li, J. Liu, L. Du, M. Chen, R. T. K. Kwok, J. W. Y. Lam, D. L. Phillips, B. Z. Tang, *Angew. Chem. Int. Ed.* **2018**, *57*, 15189–15193.
[30] K. Lee, J. Lee, E. J. Jeong, A. Kronk, K. S. J. Elenitoba-Johnson, M. S. Lim, J. Kim, *Adv. Mater.* **2012**, *24*, 2479–2484.

[31] a) C. G. Hatchard, C. A. Parker, E. J. Bowen, *Proc. R. Soc. London, Ser. A. Math. Phys. Sci.* **1956**, *235*, 518–536; b) K. Stranius, K. Börjesson, *Sci. Rep.* **2017**, *7*, 41145.
[32] a) Y. Zhao, D. G. Truhlar, *Theor. Chem. Acc.* **2008**, *120*, 215–241; b) F. Weigend, R. Ahlrichs, *Phys. Chem. Chem. Phys.* **2005**, *7*, 3297–3305.
[33] F. Neese, *WIREs Comput. Mol. Sci.* **2022**, *12*, e1606.
[34] V. Barone, M. Cossi, *J. Phys. Chem. A* **1998**, *102*, 1995–2001.
[35] A. E. Hillers-Bendtsen, J. L. Elholm, O. B. Obel, H. Hölzel, K. Moth-Poulsen, K. V. Mikkelsen, *Angew. Chem. Int. Ed.* **2023**, *62*, e202309543.

Manuscript received: April 13, 2024
Accepted manuscript online: June 2, 2024
Version of record online: July 26, 2024